

**APPENDIX E
LIMITED STRUCTURAL RECONNAISSANCE AND
PRELIMINARY PIT HIGH WALL STABILITY ASSESSMENT**

APPENDIX E LIMITED STRUCTURAL RECONNAISSANCE AND PRELIMINARY PIT HIGH WALL STABILITY ASSESSMENT

PURPOSE AND SCOPE

This appendix documents Hart Crowser's preliminary stability assessment of the North and South Pit high walls, which are relict features of the Van Stone Mine. The North Pit retains water year-round (the North Pit Lake), and the South Pit retains water seasonally. Hart Crowser assessed the stability of the North and South Pit high walls to estimate the potential for rock or slope instability that could result in failure of the North Pit Lake dam by overtopping.

Our scope of work for this task included:

- Conducting a field reconnaissance to observe and measure significant surface features relevant to rock and soil slope stability;
- Testing selected samples with a Schmidt hammer and point load apparatus to estimate rock strength index parameters;
- Evaluating the collected data to assess pit lake high wall stability; and
- Completing this appendix for the RI.

BACKGROUND INFORMATION

The Van Stone Mine is located near the contact of the Cambrian age Metaline limestone and the Spirit pluton, a granite unit of Mesozoic age. Unconsolidated glacial sediment consisting of till, outwash, and lacustrine soils overlie approximately 50 percent of the mine and surrounding area. Bedrock includes folded and faulted Paleozoic sedimentary and metasedimentary rock on side slopes and ridges of foothills and Mesozoic granitic rock on foot slopes and side slopes of foothills.

Soils in the North and South Pit areas (Area of Interest 1, or AOI-1) are of variable thickness and overlie Paleozoic metasedimentary rocks. A small amount of glacial overburden was removed to expose the ore deposits, but most of the overburden consisted of dolomitic limestone. Photographic documentation of rock structures and open pit configuration of AOI-1 are shown on Figure E-1.

Site geology is discussed further in Section 3.3 of the Remedial Investigation.

FIELD METHODS AND FINDINGS

A limited structural reconnaissance was performed at the Van Stone Mine in October 2011 and June 2012 by a field geologist and geotechnical engineer. The purpose of the reconnaissance was to observe bedrock conditions and collect data from the open pit high walls, with which to assess high wall stability.

Our efforts included measuring the spacing and orientation of fractures, noting fracture surface conditions (irregularity, weathering or alteration, infilling, and openness) and photographing field conditions. Observations were made and fracture data collected along two 50-foot transect lines in the North Pit and one in the South Pit (Figure E-2). Observations were limited to areas that were safely accessible on foot without fall protection, and then extrapolated to areas of concern. Samples from each transect were tested with a Schmidt hammer and a point load apparatus. Field methods and findings are described in the following sections.

Pit Wall Observations and Transects

The open pit high walls of both the North and South Pits are within the middle unit of the Cambrian age Metaline limestone formation, which is principally dolomite with a small amount of glacial overburden. The bedrock at all three transects (NP-T1, NP-T2, and SP-T1, shown on Figure E-2) was hard, off-white to gray, crystalline dolomitic limestone with sizeable open and filled fractures and localized banding (0.5 to 1 foot) within the massive dolomite. The most common mineral observed in fractures and on the shear surfaces was identified as brucite (Cox 1968). The observed brucite had a fibrous texture, created elongated laths, and was generally off-white to light green in color. No tremolite was observed during the limited structural reconnaissance.

Transect NP-T1

Fractures along Transect NP-T1 were typically slightly to moderately weathered¹, had very low to low persistence (the continuous length of the fracture)² (<1 to 1-3 m), and had moderately open to open fracture separation³ (0.5-2.5 to 2.5-10 mm) with slightly rough surfaces.⁴ (Refer to Table E-1 for the modified geomechanics classification [rock mass rating or RMR System]). Fractures were

¹ Refers to level of weathering on fracture surfaces in accordance to the modified RMR System.

² Refers to the continuity or persistence of a fracture in accordance to the modified RMR System.

³ Refers to aperture or separation of a fracture in accordance to the modified RMR System.

⁴ Refers to roughness of a fracture in accordance to the modified RMR System.

very pronounced along Transect NP-T1 with abundant fractured brucite fill, some residual soil, and moss within the fractures. The average fracture orientation along this transect was S40°E (140° azimuth), dipping 73° southwest. Orientations for transect NP-T1 are provided in Table E-2. A stereonet constructed from 28 recorded fractures along Transect NP-T1 is included as Figure E-3.

Note that our constructed stereonets may differ from other available references on the Van Stone Mine due, in part, to different uses of stereonets. We did not reconcile differences in our constructed stereonets.

Transect NP-T2

Fractures along Transect NP-T2 were typically slightly to moderately weathered, had very low to moderate persistence (<1 to 3-10 m), tight to moderately open fracture separation (0.1-0.5 to 0.5-2.5 mm), and slightly rough surfaces. Fractures were very pronounced along Transect NP-T2 with abundant brucite fill, some residual soil, and moss within fractures. In the middle of transect NP-T2, groundwater seepage was observed in a 6-foot section with some evidence of oxidized minerals associated with the seep. The average fracture orientation along this transect was S3°W (183° azimuth), dipping 72° northwest. Field orientations for transect NP-T2 are provided in Table E-2. A stereonet constructed from 27 observed fractures along Transect NP-T2 is included on Figure E-3.

Transect SP-T1

Fractures along Transect SP-T1 were typically fresh to moderately weathered, had very low to low persistence (<1 to 1-3 m), had moderately open to open fracture separation (0.5-2.5 to 2.5-10mm), and slightly rough surfaces (Table E-1). Fractures were very pronounced and prevalent along Transect SP-T1 with abundant brucite fill, residual soil, and moss within fractures. Transect SP-T1 was extended due to abundant soil and moss covering the open pit high wall. The average fracture orientation for this transect was S22°E (158° azimuth), dipping 72° southwest. Field orientations for transect SP-T1 are provided in Table E-2. A stereonet constructed from 61 observed fractures along Transect SP-T1 is included on Figure E-3.

Transect Summary

The bedrock along all three transects appeared generally consistent within the study area. The bedrock was hard, off-white to gray crystalline dolomitic limestone with brucite-filled fractures and localized banding (0.5 to 1 foot) within

the massive dolomite. Fractures along all three transects were typically slightly to moderately weathered, had very low to low persistence (<1 to 1-3 m), had moderately open to open fracture separation (0.5-2.5 to 2.5-10 mm), and slightly rough surfaces. Fractures were very pronounced along transects with abundant brucite filling, some residual soil, and moss within fractures. Groundwater seepage was only observed in Transect NP-T2. The average orientation of all fracture measurements taken from the three transects was S20°E (160° azimuth), dipping 72° southwest.

Site Conditions

Rock Structural Data

A summary of the structural data for the rock outcrops collected along the transects is included in Table E-2 and shown graphically as poles to planes in the stereonet, Figure E-3. The stereonet shows the clear dominant fracture orientation of steep southwest to southeast dips.

Fracture spacing, based on the three transects, averaged 1.8 and 1.9 feet at the North Pit transects (NP-T1, NP-T2) and 0.8 feet at the South Pit transect (SP-T1). Persistence of the fractures (the continuous length of the fracture) was typically up to 3 meters, but noted as high as 10 meters.

Soil Slopes

In June 2012, a field geologist walked around the perimeter of the approximately 2 acres of actively eroded exposed soils in the southwest corner of the North Pit, as shown on Figure E-1. Residual soil and glacial overburden overlie Paleozoic metasedimentary rocks (primarily dolomitic limestone) within the study area.

Soil in this area consisted of very loose to loose, damp, gravelly silty sand with occasional boulders. The exposed slopes were steep, sloping west to northwest to the North Pit Lake, with little to no vegetation as shown in Photograph 9 on Figure E-1. During the June 2012 visit, surface water was flowing into the North Pit Lake in this area.

During our reconnaissance, our field geologist looked for recent or historical evidence of soil displacement or failures such as surface cracks, scarp faces, benching, seepage, etc. No evidence of such features was observed.

ROCK STRENGTH TEST RESULTS

Outcrop samples from each transect were collected and tested with a Schmidt hammer (type L) and a point load apparatus to obtain estimates of surficial rock strength index parameters. Testing by a Schmidt hammer and point load apparatus are accepted rock mechanics testing procedures used to calculate the rock strength index. These index values are used to estimate other rock strength parameters such as uniaxial compressive strength (UCS).

Schmidt Hammer Results

In situ testing using a Schmidt impact hammer (Type L) was conducted at ten representative surface locations along each of the three transects to obtain estimates of surficial rock strength index parameters (ASTM D5873-05). Results varied by more than 100 percent. Although calculated UCS values for the massive dolomite had an average value of 6700 pounds per square inch (psi) lower bound values that probably control strength of the intact rock mass (i.e., non-kinematic failures) were less than half that value, i.e., around 3,000 psi. Schmidt hammer field measurements are provided in Table E-3.

Point Load Test Results

Fourteen representative hand samples of the massive dolomite bedrock and one representative hand sample of the abundant fracture fill, brucite, were collected at representative surface locations along each of the three transects (NP-T1, NP-T2, and SP-T1) to obtain estimates of surficial rock strength index parameters (ASTM D5731-95, Rusnak and Mark 2000). Point load test results are summarized in Table E-4. Calculated UCS values for the tested rock include:

- Massive dolomite bedrock had an average value of 2205 psi with 75 percent of the data set falling between 1680 and 2688 psi;
- The brucite fracture fill tested perpendicular to the cleavage had an average value of 2541 psi with 75 percent of the data set falling between 2142 and 3234 psi; and
- The brucite fracture fill tested parallel to the cleavage, the weakest plane, had an average value of 1092 psi with 75 percent of the data set falling between 693 and 1365 psi.

STABILITY ASSESSMENT

Since the South Pit does not have a significant lake or pit lake dam, we only evaluated the rock- and soil-slope stability of the North Pit. For the assessment, we evaluated information collected during the field reconnaissance and the estimated rock strength to assess the potential for a number of failure mechanisms of the pit high wall. The four most likely mechanisms include:

- Individual Rockfall,
- Plane Failure (Sliding Block),
- Wedge Failure; and
- Soil Slide.

Individual Rockfall

The potential for rockfalls to occur at the pits is high, based on the high wall slope angles and heights and the presence of abundant fractures that create individual blocks. The close spacing and poor persistence of the fractures (typically up to 3 meters, but noted as high as 10 meters) dictate the maximum size rock that can fall. The fracture and site characteristics indicate the potential for rocks up to about 2 feet maximum dimension to fall in a mostly vertical direction.

Plane Failure (Sliding Block)

A sliding block failure is an unusual condition that requires a number of conditions, including:

- Fracture orientation coincident with the slope face;
- Fracturing at an angle gentler than the slope face;
- Fracturing at an angle greater than the frictional strength of the rock (based on a friction-only analysis); and
- Lateral release features and fractures of sufficient persistence to allow movement of large blocks.

The persistence and orientation of observed fractures at the pits are not conducive to the occurrence of sliding blocks.

Wedge Failure

We evaluated wedge failures using the methods described in FHWA TS-89-045 (Hoek and Bray 1989). Based on the fracture data collected at the North Pit, we selected the critical joint sets listed in Table E-5.

Table E-5 - Critical Joint Sets

Transect	Joint	Strike (degrees)	Dip Direction (degrees)	Dip (degrees)
NP T-1	B	145 ⁰	235 ⁰	79 ⁰
NP T-1	A	182 ⁰	272 ⁰	70 ⁰
NP T-2	B	152 ⁰	242 ⁰	86 ⁰
NP T-2	A	190 ⁰	280 ⁰	78 ⁰

Note: Strike refers to the orientation of a fracture using compass direction, and dip gives the angle of descent below a horizontal plane.

These joint orientations were plotted on stereonet along with the orientation of the high wall face (at the North Pit) and rock strength data to evaluate wedge failure potential. The stereonet plots are included on Figure E-3. Based on the stereonet evaluations, wedge failures are possible from these joint sets and would occur at:

- NP T-1: a dip direction of 298 degrees along a 68 degrees plunge line.
- NP T-2: a dip direction of 310 degrees along a 74 degrees plunge line.

Estimating rock strength along the fracture surface as at least 30 degrees plus a joint roughness of 10 degrees, 68- and 74-degree plunges are steeper than the rock strength and less than the high wall slope, so wedge failure is a hazard.

Once sliding orientations were determined on the stereonets, we estimated the factors of safety (FS) based on simple friction-only analyses of dry slopes using Wedge Stability Charts (Hoek and Bray 1989). The charts estimate factors of safety less than 1.0 for rock slope conditions at the transect locations. Further numerical analyses corroborated these findings.

Although the average slope angle of the high wall is about 45 to 50 degrees, the benched configuration of the high wall results in near-vertical segments up to about 30 feet maximum height. These benched segments are steeper than the plunge angle of the wedge failures, so would be prone to such failures, although their extent would be limited by the bench height and the moderate persistence of the fractures. Based on the geometries of the fractures, we estimate maximum failure volumes of about 10 cubic yards in a single event. Such small volume failures are supported by wedge-shaped vacated areas in the steep benches and rock debris on the surfaces of the benches, as exhibited on Figure E-1.

Soil Slide

The southwest corner of the North Pit is an area of recent erosion and possible landsliding. The slopes in this area have thick overburden consisting of glacial till or residual soil weathered from dolomitic limestone bedrock. Unvegetated and deeply eroded slopes extend above the lake. Based on the overburden thickness, slope gradient and physical features visible in the field and in aerial photographs, landsliding appears likely to occur in this area. However, during our reconnaissance we did not observe evidence of surface tension cracks, scarp faces, benching, or groundwater seepage at the site.

CONCLUSIONS

Based on our evaluations above, we conclude that:

1. Individual rockfall hazard is high, but the resulting risk is low. Individual rocks of up to 2 feet diameter falling to the pit floor or into the lake would not generate significant waves that would overtop the tailings dam.
2. Plane failure hazard is low. The fracture orientations, low persistence, and other rock characteristics at the site do not result in a significant plane failure potential.
3. Wedge failure hazard is high above the North Pit lake. Although the hazard of wedge failure is high, the risk would only be high if a large enough failure occurred to generate waves capable of overtopping the pit lake dam. The maximum volume of wedge failure is estimated to be about 10 cubic yards. This is not a large volume, but if it occurs from one of the upper benches and is in a location that causes a wave at a vulnerable area of the dam, it could have an adverse affect on the dam. A catastrophic failure is unlikely under this scenario, but a significant erosion event leading to accelerated erosion of the pit lake dam is a reasonable concern. We estimate the risk from wedge failure to, therefore, be moderate.
4. The potential for landsliding of overburden soil in the southeast corner of the pit could not be determined. Some physical conditions suggest it has occurred in the recent past and is, therefore, likely to continue in the future but others do not support that conclusion. The risk of significant landslide hazard or risk in this area cannot be determined with the current information. However the potential for a landslide into the pit lake, and subsequent overtopping of the pit lake dam is a reasonable concern that should be further evaluated.

RECOMMENDATIONS

We recommend the following actions:

- Individual rockfalls and slab failures are not a significant risk, so no further actions are recommended.
- Wedge failures pose a moderate risk to the tailings dam. This risk should be evaluated further in the feasibility study. Evaluation should consist of first modeling the size and location of failures that could compromise the stability of the dam. Once the characteristics of such failures are known, the high wall should be evaluated for those characteristics. This additional characterization would consist of transects directly above the North Pit, and rockfall analysis of this directly collected data.
- Landslide risk at the south end of the pit could not be determined. Slumps or debris flows could deliver significant volumes of material, substantially greater than those generated by wedge failures. Their potential to generate overtopping waves could, therefore, be significant. This risk should be further assessed by more detailed geotechnical analyses and slope stability modeling.

REFERENCES

ASTM D 5731-95 Standard Test Method for Determination of the Point Load Strength Index of Rock.

ASTM D5873 - 05 Standard Test Method for Determination of Rock Hardness by Rebound Hammer Method.

Cox, M. W. 1968. Van Stone Mine Area (Lead-Zinc), Stevens County, in *Ore Deposits of the United States (The Graton-Sales Volume)*: New York, American Institution of Mining, Metallurgical, and Petroleum Engineers, v. 2, pp. 1511-1519.

Bieniawski, Z.T. 1988. The Rock Mass Rating (RMR) System (Geomechanics Classification) in *Engineering Practice, Rock Classification Systems for Engineering Purposes*, ASTM STP 984, Louis Kirkaldie, Ed. American Society for Testing and Materials, Philadelphia, 1988, pp. 17-34.

Hoek and Bray 1989. US Department of Transportation Federal Highway Administration, *Rock Slopes: Design, Excavation, Stabilization*, September 1987.

Mills, J. W., 1977 Zinc and lead ore deposits in carbonate rocks, Stevens County, Washington: Washington Division of Geology and Earth Resources Bulletin 70, 171 p.

Neitzel, T. W. 1972, Geology of the Van Stone Mine, Stevens County, Washington: Washington State University Master of Science thesis, 47 p.

Rusnak, J., and Mark, C. 2000. Using the Point Load Test to Determine the Uniaxial Compressive Strength of Coal Measure Rock. Proceedings of the 19th International Conference on Ground Control in Mining, Peng SS, Mark C, eds. Morgantown, WV: West Virginia University, 2000; 362-371

Yates, R. G.; Becraft, G. E.; Campbell, A. B.; Pearson, R. C. 1964, Tectonic framework of northeastern Washington, northern Idaho, and northwestern Montana [abstract]: American Institute of Mining, Metallurgical, and Petroleum Engineers; Canadian Institute of Mining and Metallurgy Joint Meeting, [1 p.].

L:\Jobs\1780011\Remedial Investigation Report\Final Report\Appendix E - Rock Structures and Pit Stability\Appendix E - Pit Stability.doc

Table E-1 - Geomechanics Classification

Weathering Classification of Fractures		
Grade	Symbol	Diagnostic Features
Fresh	F	No visible sign of decomposition or discoloration. Rings under hammer impact.
Slightly Weathered	WS	Slight discoloration inwards from open fractures, otherwise similar to F.
Moderately Weathered	WM	Discoloration throughout. Weaker minerals such as feldspar decomposed. Strength somewhat less than fresh rock but cores cannot be broken by hand or scraped by knife. Texture preserved.
Highly Weathered	WH	Most minerals somewhat decomposed. Specimens can be broken by hand with effort or shaved with knife. Core stones present in rock mass. Texture becoming indistinct but fabric preserved.
Completely Weathered	WC	Minerals decomposed to soil but fabric and structure preserved (Saprolite). Specimens easily crumbled or penetrated.
Residual Soil	RS	Advanced state of decomposition resulting in plastic soils. Rock fabric and structure completely destroyed. Large volume change.
Condition of Fractures (Discontinuities)		
PERSISTENCE (CONTINUITY)		
Very low (VL)		<1 m
Low (L)		1 - 3 m
Medium (M)		3 - 10 m
High (H)		10 - 20 m
Very high (VH)		> 20 m
SEPARATION (APERTURE)		
Very tight fractures (VT)		<0.1 mm
Tight fractures (T)		0.1 - 0.5 mm
Moderately open fractures (MO)		0.5 - 2.5 mm
Open fractures (O)		2.5 - 10 mm
Very wide aperture (VW)		>10 mm
ROUGHNESS (state also if surfaces are stepped, undulating or planar)		
Very rough surfaces (VR)		
Rough surfaces (R)		
Slightly rough surfaces (SR)		
Smooth surfaces (S)		
Slickensided surfaces		
ADDITIONAL COMMENTS		
Type of Filling (Gouge)		
Soil, moss, vegetation present		
Seepage		
Other distinguishing characteristics		

Note:

(1) Geomechanics classification was slightly modified from the Rock Mass Rating (RMR) System (Bienawski 1988).

Table E-2 - Strike and Dip Field Measurements

Location along Transect (in feet)	Field Strike¹ (in azimuth)	Dip² (in degrees)
North Pit Transect 1 (NP-T1)		
0.6	145	79 SW
2.0	122	66 SW
2.1	114	45 NE
2.5	190	46 SE
6.5	137	66 SW
6.9	134	70 SW
8.0	302	49 SE
9.3	119	74 NE
12.0	113	77 SW
14.0	145	53 SW
17-20.0	130	53 NW
18.0	145	68 SW
23.0	156	83 NE
24.1	156	83 NE
24.5	156	83 NE
27.4	150	82 NW
29.3	144	90
29.9-30.6	182	70 NW
32.6	169	77 NW
33.2	169	77 NW
35.4	114	87 SW
36.2	114	87 SW
36.7	114	87 SW
38-39.0	98	56 NW
41.7	141	62 NW
45.6	149	63 NW
49.1	125	73 SE
50.0	125	73 SE
North Pit Transect 2 (NP-T2)		
0.1	220	88 SE
1.2	175	58 NE
3.0	212	79 SE
4.0	212	79 SE
6.0	190	78 NW
6.2	195	75 SE
7.7	166	55 SW
7.8-9.4	220	79 SE
11.6	176	74 SW
14.5	158	66 SW
17.0	165	60 SW
18.6	175	67 NE
18.6	194	81 SE
22.0	172	90
23.5	179	69 NE
24.5	179	69 NE
25.0	143	67 NE
27.0	206	67 SE
30.4	164	90
31.3	164	90

Table E-2 - Strike and Dip Field Measurements

Location along Transect (in feet)	Field Strike¹ (in azimuth)	Dip² (in degrees)
34.2	152	86 SW
34.8	152	86 SW
38.0	147	67 SW
41.0	239	57 SE
41.5	167	79 NE
45.0	214	40 SE
46.4	212	22 SE
South Pit Transect 1 (SP-T1)		
0.8	192	71
1.1	192	71
2.2	181	72
3.1-4.0	155	77
4.0	135	75
4.9	146	76
5.3	146	76
5.7	146	76
6.1	146	76
6.3	146	76
7.0	146	76
7.0-8.1	159	60
9.4	154	63
9.6	154	63
9.9	154	63
10.4	154	63
10.7	154	63
11.0	154	63
11.4	150	72
11.4	154	63
11.9	132	70
12.4	132	70
13.0	155	71
13.5	155	71
14.4-14.9	150	60
16.0	145	78
19.2	156	61
19.3	160	73
20.0	180	75
20.9	145	59
21.4	169	62
22.7	182	72
22.8	182	72
22.9	182	72
24.0	182	72
25.4	157	73
25.8	157	73
26.3	157	73
27.1	157	73
27.8	157	73
29.2	157	73
29.9	157	73

Table E-2 - Strike and Dip Field Measurements

Location along Transect (in feet)	Field Strike¹ (in azimuth)	Dip² (in degrees)
30.8	183	86
31.0	183	86
31.9	183	86
32.8	183	86
33.5	190	60
35.4	210	77
36.2	210	77
38.1	210	77
39.0	157	79
39.5	157	79
40.3	145	66
40.9	145	66
47.0	100	63
47.3	145	79
47.9	145	79
48.2	145	79
53.0	90	60
54.0	90	60
57.0	90	60

Notes:

1. Strike refers to the orientation of a fracture using compass direction.
2. Dip gives the angle of descent below a horizontal plane.

Table E-3 - Schmidt Hammer Field Measurements

Measurement ID	Schmidt Hammer Rebound
<i>North Pit Transect 1 (NP-T1)</i>	
1	32
2	58
3	46
4	34
5	48
6	43
7	38
8	52
9	34
10	38
<i>North Pit Transect 2 (NP-T2)</i>	
1	29
2	50
3	22
4	48
5	46
6	50
7	38
8	38
9	32
10	23
<i>South Pit Transect 1 (SP-T1)</i>	
1	42
2	22
3	31
4	38
5	38
6	36
7	27
8	32
9	34

Notes:

Field measurements were collected with a Type L Schmidt hammer, based on ASTM D5873 - 05. Rebound measurements (R) are corrected for horizontal orientation.

Table E-4 - Point Load Test Results

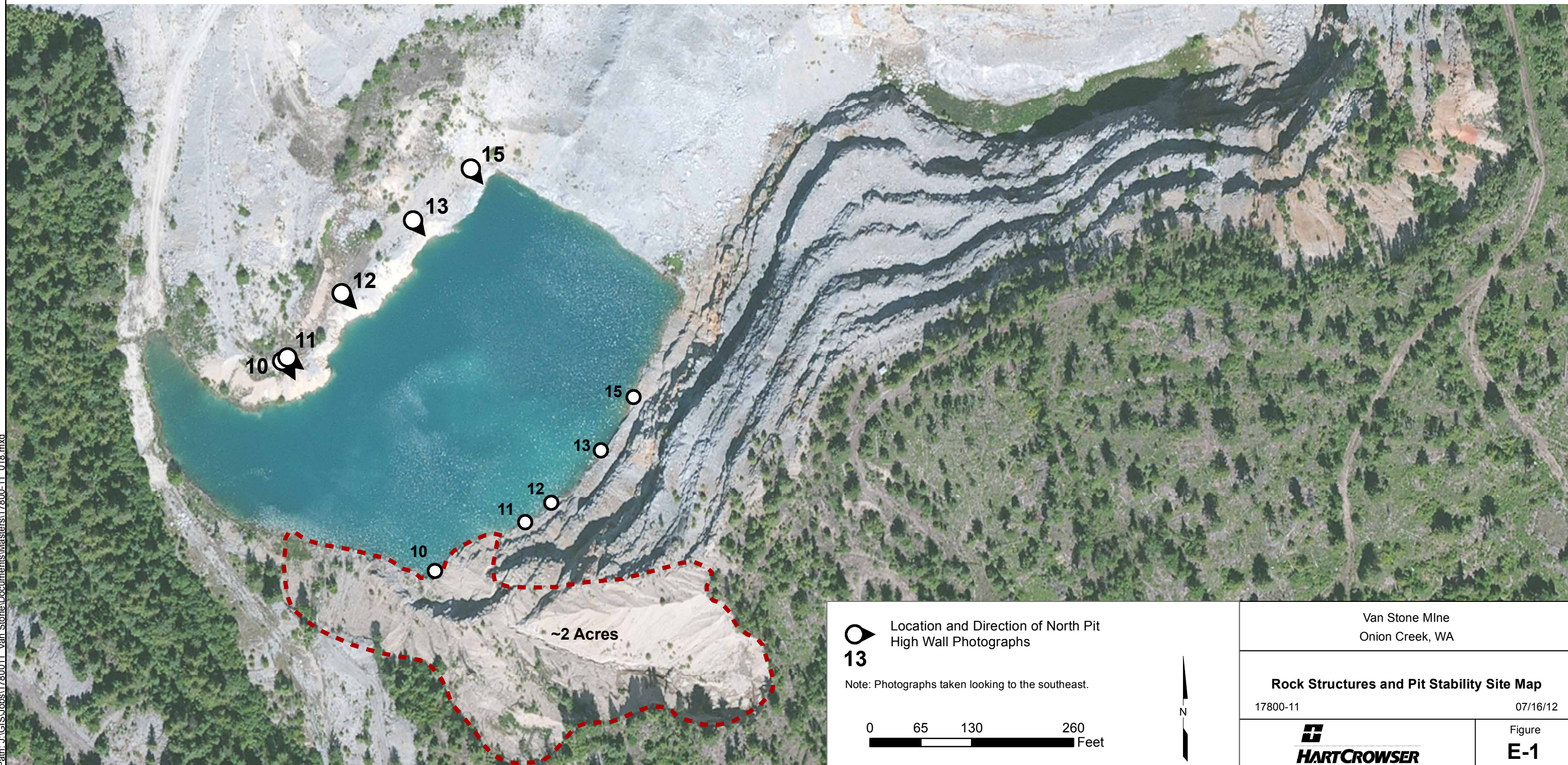
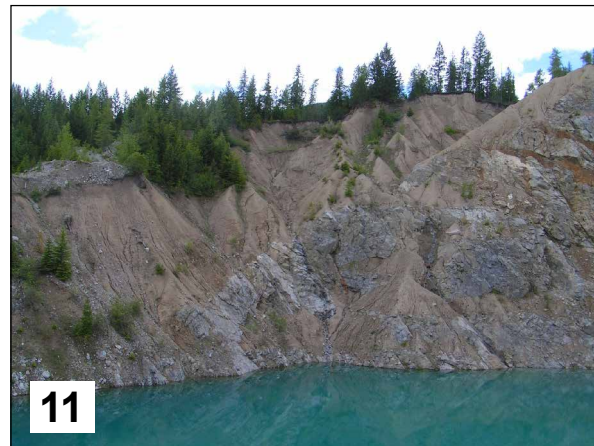
Rock Sample	# Values in Data Set (N)	Units (PSI)	Minimum (0 %)	25%	50%	75%	Maximum (100%)
Massive Dolomite Bedrock	24	UCS	1008	1680	2205	2688	6048
Brucite Fill perpendicular to cleavage	19	UCS	1512	2142	2541	3234	4263
Brucite Fill parallel to cleavage	22	UCS	357	693	1092	1365	2079

Notes:


N - Number of values in data set.

PSI - pounds per square inch.

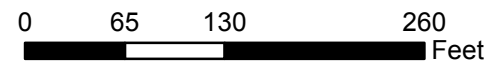
UCS - Uniaxial compressive strength.



Path: J:\GIS\Jobs\1780011_Van Stone\Documents\Masters\17800-11_018.mxd


 Location and Direction of North Pit High Wall Photographs
13

Note: Photographs taken looking to the southeast.



Van Stone Mine
Onion Creek, WA

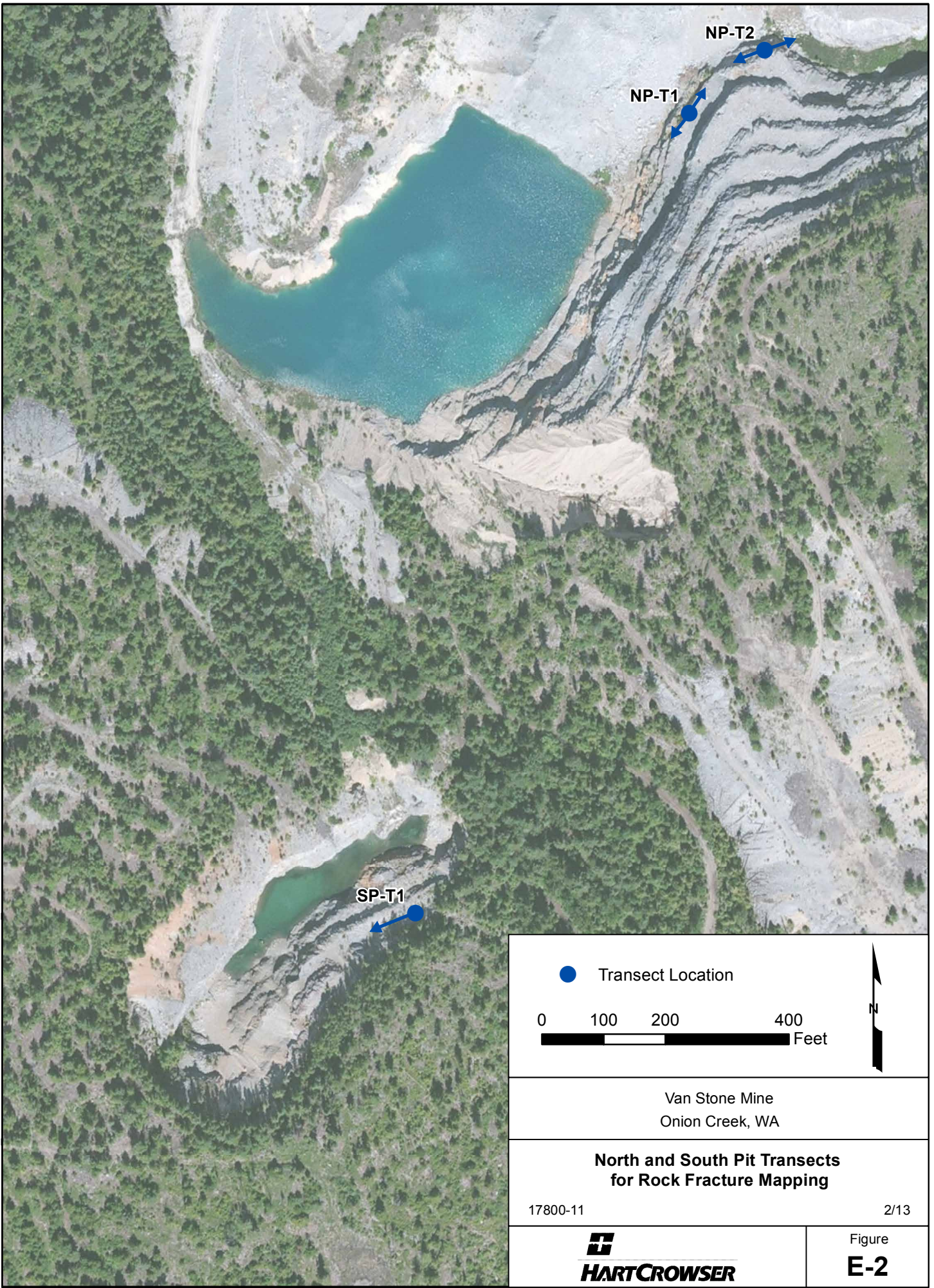
Rock Structures and Pit Stability Site Map

17800-11

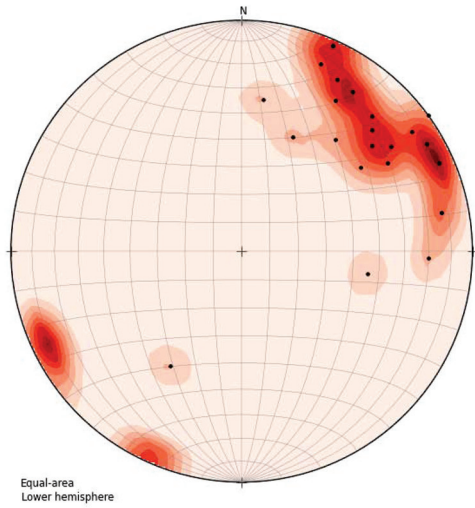
07/16/12



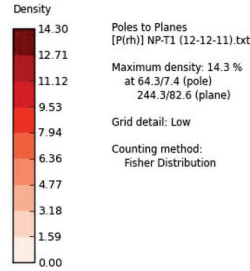
Figure
E-1



A. Poles from NP-T1

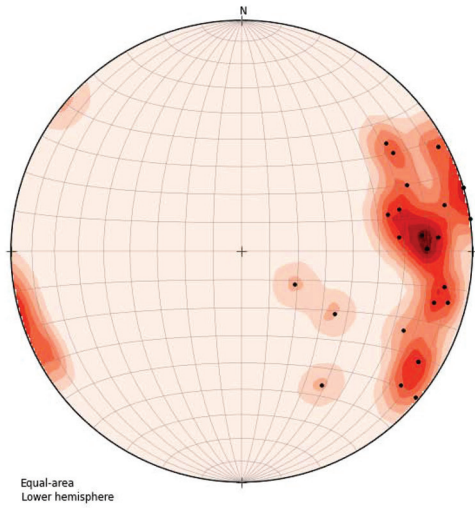


• [P(rh)] NP-T1 (12-12-11).txt (poles to planes) n=28

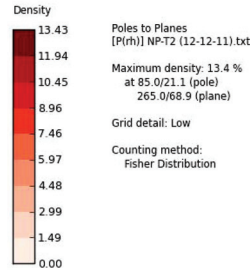


Equal-area
Lower hemisphere

B. Poles from NP-T2

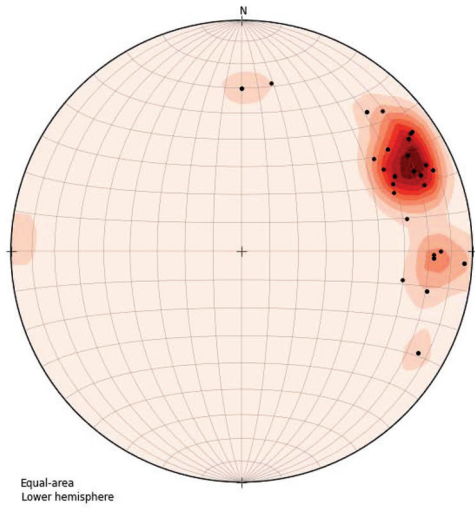


• [P(rh)] NP-T2 (12-12-11).txt (poles to planes) n=27

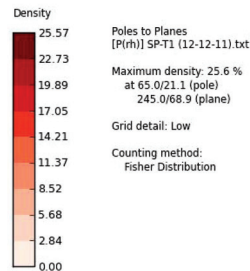


Equal-area
Lower hemisphere

C. Poles from SP-T1



• [P(rh)] SP-T1 (12-12-11).txt (poles to planes) n=61



Equal-area
Lower hemisphere

Van Stone Mine
Onion Creek, WA

**Stereonets Constructed from Poles to Planes
in the North and South Pit Transects**

17800-11

2/13



Figure

E-3